High second-order nonlinearities in poled silicate fibers

P. G. Kazansky, L. Dong, and P. St. J. Russell

Optoelectronics Research Centre, University of Southampton, Southampton S09 5NH, UK

Received December 20, 1993

Effective quadratic nonlinearities as high as 0.2 pm/V are reported for the first time to our knowledge in poled germanosilicate fibers. This value is ~200 times higher than previously achieved in these fibers. The presence of Ge is found to enhance the efficacy of both thermal (in combination with OH doping) and electron-beam poling in silica.

Recently high second-order nonlinearities of the order of 1 pm/V were observed in glasses by a variety of different techniques: thermal poling,[1] corona poling,[2] and electron implantation.[3] These observations have excited considerable interest[4–7] because they offer the prospect of linear electro-optic modulators and parametric frequency converters monolithically integrated into optical fibers or planar glass waveguides. However, to our knowledge there have not yet been any reports of successful poling of optical fibers. The maximum second-order nonlinearities obtained by seeding with light,[8] poling with a high electrical field in germanosilicate fibers,[9] and excitation poling in P-doped germanosilicate fibers[10] remain, respectively, 3 orders and 1 order of magnitude lower than the thermal poling value of 1 pm/V.

In this Letter we report what is to our knowledge the first successful poling of optical fiber with both thermal and electron implantation techniques. Compared with previous research in germanosilicate fibers a 200-fold improvement in second-order nonlinearity is obtained.

In the first stage of our experiments, fiber performs with different compositions were thermally poled to identify the best core and cladding compositions and to help understand the underlying mechanism. The preforms investigated are listed in Table 1. Slices approximately 1 mm thick from each preform were thermally poled at 2.5-kV applied voltage and 280 °C temperature for 15 min in an oven. Stainless-steal and Si electrodes were used.

After poling, the electrodes were removed, and the samples were tested for evidence of second-harmonic (SH) generation. Q-switched and mode-locked pulses from a Nd:YAG laser operating at 1064 nm were used as the pump source. The laser beam was focused to a spot size of ~50 μm (using a lens with focal length 10 cm) onto the anodic surface. The angle of incidence (~60°) was chosen to lie close to the Brewster angle. After crossing the sample, the diverging laser radiation was focused with a second lens onto a separate detectors for pump and SH light. The SH signal was monitored while the sample was translated in a direction perpendicular to the plane of incidence. No SH signal was detected in any region of preforms A and E. In contrast, a strong SH signal was observed in the starting tube of preforms B, C, and D, and no SH signal was observed in the P + F-doped cladding while the p-polarized pump beam was scanned along preform B (Fig. 1). A small peak in the SH signal was also observed at the boundary between the starting tube and the cladding with s-polarized pumping. This may be explained by the existence of a fringing electrostatic field at the boundary between the two regions. This has been confirmed by the observation of a peak in the SH signal at the boundary while the pump beam was scanned (at normal incidence) along the surface of the sample. We observed an ~15% stronger SH signal in the Ge-doped core compared with that in the starting tube (Fig. 2). The SH signal in the core was also found to follow the Ge concentration. The measured absorption spectrum in the core region of performs C and D indicated an OH concentration of ~80 parts in 10^6 (ppm).

Our results may be explained by the high H^+ content in the starting tubes and the preform core, where they act as positively charged carriers; interestingly, Na doping (perform D) produced no significant effect on the SH signal. The latter result may be explained by saturation of the internal electrostatic field in the region depleted of H^+ ions. Na^+ ions may act as cations and lead to a poling effect in Na-doped silica glass in the absence of H^+ doping. The observation of a higher SH signal in the Ge-doped cores may be due to the Ge defect sites, which can be relatively more easily ionized by the high electrostatic field in the H^+ depletion region near the anode, creating a frozen-in electric field.

For the fiber poling experiments, preform B and a preform similar to preform C (GeO_2 concentration ~1.5 times less then in preform C) were pulled into fiber B (core diameter 2 μm, outer diameter 100 μm, numerical aperture 0.27) and fiber C (core diameter 16 μm, outer diameter 125 μm, numerical aperture 0.09), respectively. Regions ~8 mm long were side polished to within ~1 μm of the core. We used a simple wheel polishing technique,[11] which takes only a few minutes and induces no detectable additional loss. The side-polished fibers were placed on top of a 2-mm-thick silica substrate manufactured by the same method as the starting tubes (Herasil 1), and the final assembly was sandwiched between two electrodes with the anodic electrode on top of the polished

0146-9592/94/100000-03$6.00/0

Table 1. Summary of Fiber Preforms Tested by Thermal Poling

Preform (Type)[a]	Glass Tube			Inner Cladding	Core
	Type[b]	Name	OH Concentration (ppm)		
A (MCVD)	EFNQ	GE-100	~1	P + F-doped silica	3.5 mol. % GeO_2
B (MCVD)	FFNQ	Herasil 1	~150	P + F-doped silica	18 mol. % GeO_2 + Na
C (MCVD)	FFNQ	Herasil 1	~150	–	3.9 mol. % GeO_2
D (MCVD)	FFNQ	Herasil 1	~150	–	4.5 mol. % GeO_2 + Na
E (VAD)	–	–	~40	–	8 mol. % GeO_2

[a]MCVD, modified chemical-vapor deposition; VAD, vapor axial deposition.
[b]EFNQ, electrically fused natural quartz; FFNQ, flame-fused natural quartz.

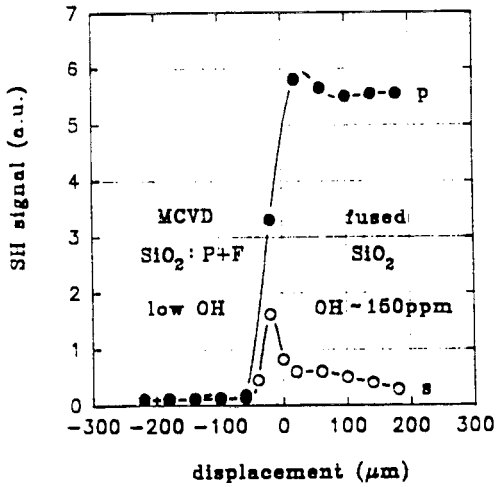

Fig. 1. SH signals for the *p*-polarized pump (●) and the *s*-polarized pump (○) in the cladding and the starting tube in preform B.

fiber surface (Fig. 3). Thermal poling was carried out at 4.3 kV and 280 °C for 15 min.

After thermal poling, pump light was launched into the fibers. No SH signal was seen in fiber B. In contrast, a strong non-phase-matched SH signal (visible to the naked eye) was observed in fiber C. We obtained a conversion efficiency of 3×10^{-6} % at an infrared pump power of ~1 kW. Taking into account the fact that the SH signal is generated at half the coherence length [$\Lambda_{coh}/2 = \lambda/4(n^*_{2\omega} - n^*_{\omega}) \simeq 20$ μm, where $\lambda = 1064$ and $n^*_{2\omega}$ and n^*_{ω} are the effective indices of the SH and infrared fiber modes (Ref. 12)], we estimated the effective value of the induced second-order susceptibility [$X^{(2)}_{eff} = X^{(2)}\eta$, where η is the overlap integral between the nonlinearity and the modal field] to be ~ 0.2 pm/V. Because the fiber geometry is more complicated, exact measurements of the thickness and location of the nonlinear layer are difficult. Nevertheless, if we assume the thickness of the nonlinear layer to be ~7 μm,[7] the value of the overlap factor for our fiber is $\eta \leq 0.4$, which yields a value of $X^{(2)} \geq 0.5$ pm/V.

Experiments on electron-beam poling were also carried out in a Ge-doped fiber preform (preform E), a side-polished Ge-doped fiber (core diameter 4 μm, outer diameter 90 μm, numerical aperture 0.3) with 22.7 mol. % GeO_2, and a pure silica sample (Suprasil). Samples were irradiated in a scanning electron microscope at 0.3-nA beam current and 40-kV beam voltage. The TV mode of the scanning electron microscope (horizontal scanning rate 0.064 ms/line, vertical scanning rate 20 s/frame) was used. Areas of approximately 1 mm^2 and 0.01 mm^2 on the surfaces of bulk and fiber samples, respectively, were irradiated for 1 min. After irradiation, the samples were

Au: see msp. 10.

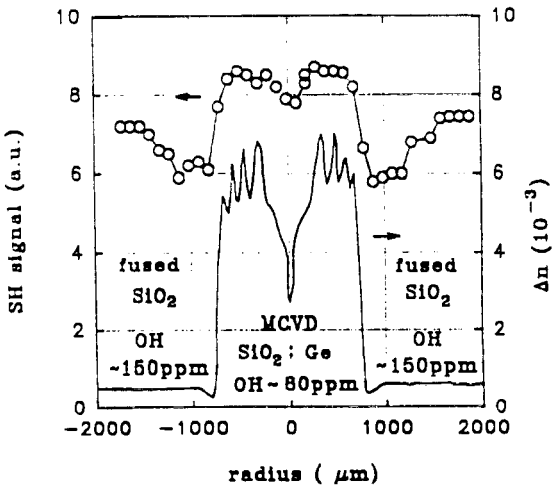

Fig. 2. SH signal (○) and refractive-index difference (solid curve) in preform C.

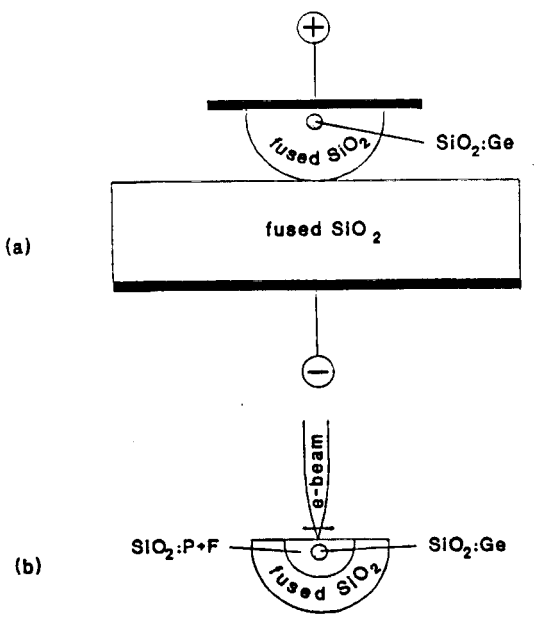

Fig. 3. (a) Thermal and (b) electron-beam poling arrangements for the fibers.

tested for evidence of SH generation by probe technique developed for thermally poled samples. No SH signal was registered in the irradiated pure silica sample. Values of $\chi^{(2)} \simeq 0.2$ pm/V and $\chi^{(2)}_{\text{eff}} \simeq 0.1$ pm/V, respectively, were obtained in the core region of the Ge-doped preform and in the fiber. The result obtained with electron-beam poling of Ge-doped silica can be explained by Ge-related defect centers, which act as traps for implanted electrons and also may cause an increase in secondary electron emission that finally leads to an increase in the built-in electrostatic field.

In conclusion, Ge-doping is observed to enhance both thermal poling (in combination with OH doping) and electron-beam poling effects. Ge-related defect centers, similar to those which cause photosensitivity in Ge-doped fibers, may be responsible for this. Values of effective $\chi^{(2)}$ as high as 0.2 pm/V have been obtained in these fibers. This value may be increased by improvement in the overlap integral between the nonlinear layer and the fiber modal field. With the polishing technique used, arbitrarily long fiber regions can easily be side polished and poled. Perhaps the most significant conclusion is that, despite the relatively complex structure of pulled optical fiber (different regions with different properties, small dimensions, etc.), successful application of the new poling technologies developed for planar structures is fairly straightforward. Experiments on $\chi^{(2)}$ grating fabrication in poled fibers are currently in progress.

The authors are grateful to P. Hua for preparation of the polished samples, to J. Minelly for advice on the side-polishing technique, and to B. Ault and B. Cressey for their help in electron-beam irradiation of the samples. This study was supported by the U.S. Department of the Air Force through the European Office of Aerospace Research and Development, London.

References

1. R. A. Myers, N. Mukherjee, and S. R. J. Brueck, Opt. Lett. **16,** 1732 (1991).
2. A. Okada, K. Ishii, K. Mito, and K. Sasaki, Appl. Phys. Lett. **60,** 2853 (1992).
3. P. G. Kazansky, A. Kamal, and P. St. J. Russell, Opt. Lett. **18,** 693 (1993).
4. H. Nasu, H. Okamoto, A. Mito, J. Matsuoka, and K. Kamiya, Jpn. J. Appl. Phys. **32,** 406 (1993).
5. K. Tanaka, K. Kashima, K. Hirao, N. Soga, A. Mito, and H. Nasu, Jpn. J. Appl. Phys. **32,** 843 (1993).
6. A. C. Liu, M. J. F. Digonnet, and G. S. Kino, in *Integrated Photonics Research,* vol. 10 of 1993 OSA Technical Digest Series (Optical Society of America, Washington, D.C., 1993), paper PD6.
7. P. G. Kazansky, A. Kamal, and P. St. J. Russell, Opt. Lett. **18,** 1141 (1993).
8. U. Österberg and W. Margulis, Opt. Lett. **11,** 516 (1986).
9. L. Li and D. N. Payne, in *Integrated and Guided-Wave Optics,* Vol. 4 of 1989 OSA Technical Digest Series (Optical Society of America, Washington, D.C., 1989), paper TuAA2.
10. M.-V. Bergot, M. C. Farries, L. Li, L. J. Poyntz-Wright, P. St. J. Russell, and A. Smithson, Opt. Lett. **13,** 592 (1988).
11. C. D. Hussey and J. D. Minelly, Electron. Lett. **24,** 805 (1988).
12. R. Kashyap, J. Opt. Soc. Am. B **6,** 313 (1989).